

## Templated Carbon Nanofiber with Mesoporosity and Semiconductivity

Weon-Sik Chae,<sup>†</sup> Myoung-Jin An,<sup>†</sup> Sang-Wook Lee,<sup>†</sup> Min-Soo Son,<sup>‡</sup> Kyung-Hwa Yoo,<sup>\*,‡</sup> and Yong-Rok Kim<sup>\*,†</sup>

Photon Applied Functional Molecule Research Laboratory, Department of Chemistry, Yonsei University, Seoul 120-749, South Korea, and Department of Physics, Yonsei University, Seoul 120-749, South Korea

Received: January 16, 2006; In Final Form: February 16, 2006

We have newly fabricated a long one-dimensional (1D) mesoporous carbon nanofiber by using a mesoporous silica nanofiber template. The resulting mesoporous carbon nanofiber shows the unique mesoporous structure of circularly wound nanochannel alignment perpendicular to the long fiber axis and the high gas sorption property, which interestingly presents the *p*-type semiconducting behavior.

Since the fullerene<sup>1</sup> and carbon nanotubes,<sup>2</sup> carbon materials have attracted much attention in the fields of chemistry, physics, and material science and engineering because of their unique structural and energetic properties. These properties are distinct from those of the conventional carbon allotropes of diamond and graphite.<sup>3</sup> To date, the carbon materials have been prepared in various morphologies, such as spherical and elongated balls (C<sub>60</sub>, C<sub>70</sub>, C<sub>78</sub>, etc.),<sup>4</sup> one-dimensional (1D) tubes (single-walled and multiwalled carbon nanotubes),<sup>5</sup> mesoporous carbon networks (CMK-1, CMK-3, etc.),<sup>6,7</sup> and conventional carbon materials.<sup>8,9</sup> Among the carbon materials, 1D carbon nanomaterials show great potential for energy storage, electronic devices, and molecular sensors because of their unique electronic properties, excellent mechanical strength, and high chemical stability.<sup>10</sup>

Recently, mesoporous carbon (MC), another type of the carbon material, has been studied extensively.<sup>6,7,11–15</sup> Most of the MCs were prepared by the templating method with mesoporous silica materials. Because the resulting MC materials usually possessed the properties of high specific surface area and gas permeability,<sup>6,11</sup> they could be utilized as a hydrogen storage medium or catalyst.<sup>11,12</sup> So far, the majority of these MC materials have been fabricated as bulk materials.<sup>11–13</sup> Because the 1D morphology has high potential for practical applications, several studies have been tried previously to fabricate porous microfibers by using conventional extrusion methods or solution systems.<sup>12,14</sup> The fabricated fibrous MCs, however, did not exhibit well-controlled morphologies in either macro- or microscopic structures.

Very recently, 1D silica nanofibers with mesoporous internal structures have been developed through two methods; the confinement-induced mesoscopic self-assembly of the surfactant and the silica sol within the porous templates<sup>16,17</sup> or the direct mesoscopic self-assembly of the surfactant and the silica sol in

acidic solutions.<sup>18</sup> The resultant mesoporous silica nanofibers are hexagonally packed and possess prominent gas-adsorption characteristics. The internal nanochannel structures of the mesoporous silica nanofibers can generally be classified by two features: the nanochannel alignment parallel to the long fiber axis and the circularly wound nanochannel alignment perpendicular to the long fiber axis.<sup>17,18</sup>

In this study we have newly synthesized a long 1D MC nanofiber with a typical length of 10–30  $\mu\text{m}$  by applying a templating method. The mesoporous silica nanofiber with the internal mesostructure of circularly wound nanochannel alignment was used as a structure-directing template for the preparation of the 1D MC nanofiber. The MC nanofiber was replicated by filling the mesoporous silica nanofiber template with a carbon source and subsequent polymerizing, carbonizing, and removing the silica template. The resulting MC nanofiber shows a well-organized internal mesostructure. Moreover, the single MC nanofiber displays a *p*-type semiconducting behavior.

The detailed preparation procedures are as follows. The mesoporous silica nanofiber template was prepared within porous alumina membrane (PAM) support, similar to previous reports (Supporting Information)<sup>16</sup> because this templating method has the advantage of precision control of diameter (20–300 nm) and length (0.1–100  $\mu\text{m}$ ) as well as a well-aligned feature of the silica nanofibers compared with the direct solution method. Before carbon replication, the block copolymers incorporated within the mesoporous silica nanofibers were removed by calcination for 4 h at 450 °C. Also, the hybrid template of mesoporous silica nanofibers within PAM was doped with aluminum atoms. It was accomplished by dipping the hybrid membrane into 30 mL of solution containing 0.02 M AlCl<sub>3</sub> (98%, Junsei Chemical Co., Japan) ethanol solution for 4 h followed by heating at 550 °C for 2 h. This process provided the solid acid sites to initiate the polymerization of furfuryl alcohol (99%, Aldrich; FA). The hybrid template was infiltrated with FA molecules by incipient wetness under a vacuum condition (<10<sup>-2</sup> Torr) at room temperature for 2 h. The FA filled within the hybrid membranes was polymerized by heating overnight at 90 °C, followed by heating for 6 h at 350 °C under argon flow. To increase the amount of FA that

\* Corresponding authors. (Y.-R.K) Telephone: +82 (0)2 2123 2646. Fax: +82 (0)2 364 7050. E-mail: yrkim@yonsei.ac.kr; (K.-H.Y) Telephone: +82 (0)2 2123 3887. Fax: +82 (0)2 392 1592. E-mail: khyoo@yonsei.ac.kr.

<sup>†</sup> Department of Chemistry, Yonsei University.

<sup>‡</sup> Department of Physics, Yonsei University.

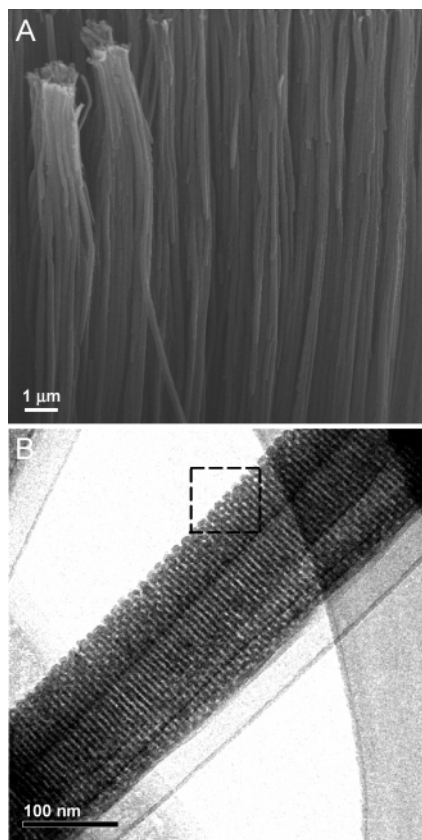


**Figure 1.** (A) FE-SEM and (B) TEM images of the MC nanofiber replicated from the mesoporous silica nanofiber with the internal mesostructure of circularly wound nanochannel alignment perpendicular to the long fiber axis. The images were obtained after the complete removal of the hybrid template of the mesoporous silica nanofibers within porous alumina by a hydrofluoride (HF) aqueous solution.

could be stored within the nanochannels of the mesoporous silica nanofibers, the processes of the FA filling and polymerization were repeated two times. The carbonization of the hybrid membrane filled with the polymerized FA was conducted in a temperature-controlled furnace at 700 °C for 2 h under argon flow.

The hybrid template of the mesoporous silica nanofibers within PAM was removed completely by a diluted HF (5 wt %) aqueous solution in order to investigate the detailed morphology and the internal mesostructure of the resulting carbon nanomaterial. For the measurements of electrical transport properties, the MC nanofiber was dispersed in ethanol and then spin-coated onto a degenerately doped Si substrate with a thermally grown 500-nm-thick SiO<sub>2</sub> layer. The MC nanofiber was located by a field emission scanning electron microscope (FE-SEM), and Au/Ti electrodes were deposited by using the electron beam lithography and lift-off techniques, as shown in the upper inset of Figure 4. Rapid thermal annealing was performed at 500 °C for 2 min in a vacuum ( $\sim 10^{-3}$  Torr) in order to have good contacts between a single MC nanofiber and the metal electrodes.<sup>19</sup>

The transmission electron microscope (TEM) image shows that the mesoporous silica nanofiber used as a template in this study has the well-organized unique mesoporous internal structure of circularly wound nanochannel alignment perpendicular to the long fiber axis (Supporting Information, Figure S1). After the carbonization and complete removal of the hybrid template (the mesoporous silica nanofibers within PAM), the resulting replicated carbon nanomaterial appears to be the long

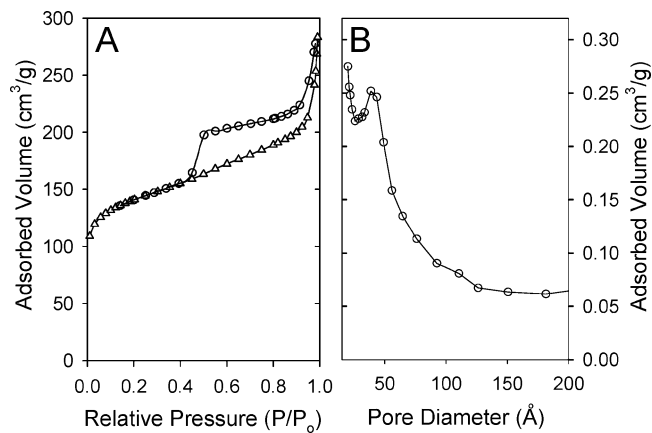


**Figure 2.** (A) Nitrogen gas adsorption–desorption isotherm and (B) pore diameter distribution of the MC nanofiber. The pore diameter distribution is estimated by applying a Barrett–Joyner–Halenda (BJH) method to the adsorption branch.

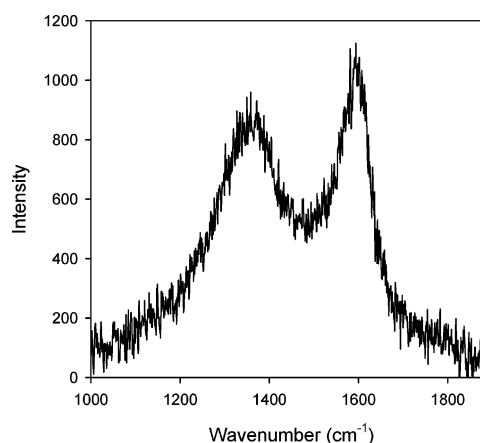


**Figure 3.** Raman spectrum of the MC nanofiber.

fibers that are vertically assembled, as shown in Figure 1A. The typical diameter and length of the mesoporous carbon nanofibers are 150–300 nm and 10–30  $\mu\text{m}$ , respectively. Such assembled carbon nanofibers were dispersed easily in ethanol and, therefore, a single carbon nanofiber could be applied for the measurements of TEM and electrical conductivity. Figure 1B reveals that the resulting MC nanofiber has a well-organized internal mesostructure. This MC nanofiber shows the internal mesostructure with the negative replication image of the mesoporous silica nanofiber template: each component carbon nanochannel exhibits void channel structure, which is a CMK-5 typed tubular nanochannel, as shown in the selected area of Figure 1B.

Figure 2 shows the nitrogen gas adsorption–desorption isotherm for the MC nanofiber. This isotherm exhibits a characteristic hysteresis behavior, which is typically observed in bulk MC materials.<sup>20</sup> The Brunauer–Emmett–Teller (BET) surface area, pore volume, and pore diameter are estimated to be 489.3 m<sup>2</sup>/g, 0.37 m<sup>3</sup>/g, and 38.7 Å for the MC nanofiber, respectively. However, a hysteresis loop is additionally observed above the partial pressure of 0.9, which is possibly due to interstitial spaces among the MC nanofibers. Furthermore, one notable point is that the estimated surface area and the pore volume of the MC nanofiber are much lower than those values of the bulk MC materials that have been reported in reference 20. These observed lower values seem to be responsible for the structural uniqueness, that is, the circularly wound nano-

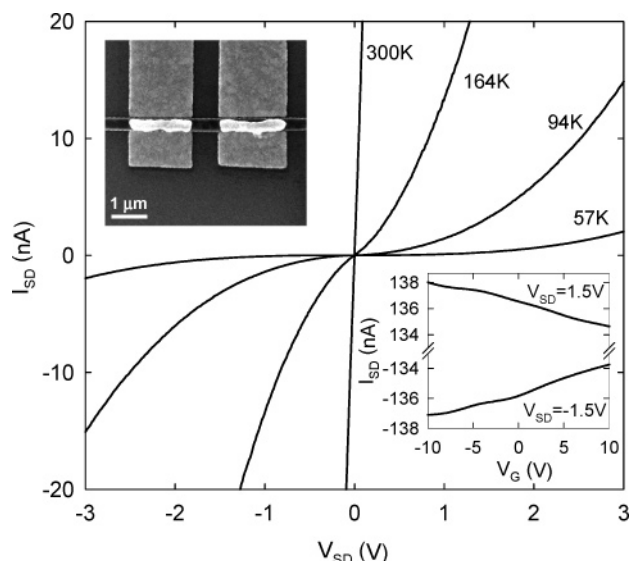


**Figure 4.** Temperature-dependent source/drain current–voltage ( $I_{SD}$ – $V_{SD}$ ) curves of the MC nanofiber. The upper inset is the FE-SEM image of a representative MC nanofiber device. The lower inset is the source/drain current–gate voltage ( $I_{SD}$ – $V_G$ ) curves for the corresponding device.

channel alignment perpendicular to the long fiber axis, with the nanochannels of closed void ring (Figure 1B).

The Raman spectrum shows two characteristic vibration modes at  $\sim 1340$  and  $\sim 1590$   $\text{cm}^{-1}$  (Figure 3) for the MC nanofiber. According to the literature on carbon materials,<sup>21,22</sup> the former vibration mode was typically observed when reducing the cluster size of carbon material, which induces a breathing mode ( $A_{1g}$  symmetry, D-mode), whereas the latter originated from the characteristic tangential mode of carbon material ( $E_{2g}$  symmetry, G-mode). The intensity ratio of D-mode to G-mode is inversely related to the cluster diameter ( $L_a$ ) according to the following relationship:  $I_D/I_G = C(\lambda)/L_a$ , where the  $C(\lambda)$  is the scaling factor of  $\sim 44$  Å using a laser excitation source of 514.5 nm.<sup>22</sup> The observed intensity ratio ( $I_D/I_G$ ) is shown to be  $\sim 0.92$  for the MC nanofiber. From this intensity ratio, the average cluster diameter ( $L_a$ ) of the carbon constituent is estimated to be  $\sim 48$  Å. Therefore, it implies that the fabricated MC nanofiber consists primarily of carbon nanoclusters.

Figure 4 shows the source/drain current–voltage characteristics ( $I_{SD}$ – $V_{SD}$ ) measured at several temperatures for a single MC nanofiber. As temperature decreases, conductance decreases and the voltage gap widens. In the lower inset of Figure 4, the current measured with the constant  $V_{SD}$  is plotted as a function of the back-gate voltage. The conductance decreases with increasing gate voltage, which indicates that the MC nanofiber exhibits the  $p$ -type semiconducting behavior. The electrical transport measurements on more than 12 devices were repeated, and similar behaviors were observed for all of the devices. Because the MC nanofiber consists primarily of carbon nanoclusters, the semiconductive properties are possibly due to the mesoscopically aggregated carbon nanoclusters within the MC nanofiber.

In summary, we have newly fabricated a long MC nanofiber, which consists mainly of carbon nanoclusters, by using a mesoporous silica nanofiber template. The resulting MC nanofiber presents the unique mesoporous structure of circularly wound nanochannel alignment perpendicular to the long fiber axis and high gas sorption property. In particular, the MC nanofiber shows the  $p$ -type semiconducting behavior. Because of their unique semiconducting behavior, the 1D MC nano-

material can be applied potentially in the field of molecular electronic devices.

**Acknowledgment.** This work is financially supported by a grant from the National Research Laboratory (NRL) (grant no. M1-0302-00-0027) program administered by the Ministry of Science and Technology (MOST) and a Yonsei Center for Studies on Intelligent Biomimic Molecular Systems. We are grateful for instrumental supports from the equipment facility of CRM-KOSEF, Korea University. Prof. K.-H.Y. is thankful for a grant from National Core Research Center for Nanomedical Technology administered by the Korea Science and Engineering Foundation (KOSEF).

**Supporting Information Available:** Experimental details and TEM image of the mesoporous silica nanofiber template, instrumentation details, and energy-dispersive X-ray spectrum of the mesoporous carbon nanofiber. This material is available free of charge via the Internet at <http://pubs.acs.org>.

## References and Notes

- (1) Kroto, H. W.; Leath, J. R.; O'Brien, S. C.; Curl, R. F.; Smalley, R. E. *Nature* **1985**, *318*, 162.
- (2) Iijima, S. *Nature* **1991**, *354*, 56.
- (3) (a) Harris, P. J. F. *Carbon Nanotubes and Related Structures*; Cambridge University Press: Cambridge, 1999. (b) Dresselhaus, M. S.; Dresselhaus, G.; Avouris, Ph. *Carbon Nanotubes: Synthesis, Structure, Properties, and Applications*; Springer-Verlag: Berlin, 2001. (c) Dai, H. *Acc. Chem. Res.* **2002**, *35*, 1035.
- (4) (a) Taylor, R.; Hare, J. P.; Abdul-Sada, A. K.; Kroto, H. W. *J. Chem. Soc., Chem. Commun.* **1990**, 1423. (b) Johnson, R. D.; Meijer, G.; Salem, J. R.; Bethune, D. S. *J. Am. Chem. Soc.* **1991**, *113*, 3619. (c) Sun, G.; Kertesz, M. *J. Phys. Chem. A* **2000**, *104*, 7398.
- (5) (a) Jeong, S.-H.; Ko, J.-H.; Park, J.-B.; Park, W. *J. Am. Chem. Soc.* **2004**, *126*, 15982. (b) Pan, Z. W.; Xie, S. S.; Chang, B. H.; Wang, C. Y.; Lu, L.; Liu, W.; Zhou, W. Y.; Li, W. Z.; Qian, L. X. *Nature* **1998**, *394*, 631.
- (6) (a) Ryoo, R.; Joo, S. H.; Jun, S. *J. Phys. Chem. B* **1999**, *103*, 7743. (b) Jun, S.; Joo, S. H.; Ryoo, R.; Kruk, M.; Jaroniec, M.; Liu, Z.; Ohsuna, T.; Terasaki, O. *J. Am. Chem. Soc.* **2000**, *122*, 10712.
- (7) Liang, C.; Hong, K.; Guiochon, G. A.; Mays, J. W.; Dai, S. *Angew. Chem., Int. Ed.* **2004**, *43*, 5785.
- (8) Marsh, H. *Introduction to Carbon Science*; Butterworth: London, 1989.
- (9) Harris, P. J. F. In *Chemistry and Physics of Carbon*; Radovic, L. R., Ed.; Marcel Dekker: New York, 2003; Vol. 28, Chapter 1.
- (10) (a) Kong, J.; Franklin, N. R.; Zhou, C.; Chapline, M. G.; Peng, S.; Cho, K.; Dai, H. *Science* **2000**, *287*, 622. (b) Kong, J.; Yenilmez, E.; Tomblar, T. W.; Kim, W.; Dai, H.; Laughlin, R. B.; Liu, L.; Jayanthi, C. S.; Wu, S. Y. *Phys. Rev. Lett.* **2001**, *87*, 106801. (c) Javey, A.; Guo, J.; Wang, Q.; Lundstrom, M.; Dai, H. *Nature* **2003**, *424*, 654.
- (11) Joo, S. H.; Choi, S. J.; Oh, I.; Kwak, J.; Liu, Z.; Terasaki, O.; Ryoo, R. *Nature* **2001**, *412*, 169.
- (12) Shinkarev, V. V.; Fenelonov, V. B.; Kuvshinov, G. G. *Carbon* **2003**, *41*, 295.
- (13) Kuno, M.; Naka, T.; Negishi, E.; Matsui, H.; Terasaki, O.; Ryoo, R.; Toyota, N. *Synth. Met.* **2003**, *135–136*, 721.
- (14) (a) Ozaki, J.; Endo, N.; Ohizumi, W.; Igarashi, K.; Nakahara, M.; Oya, A.; Yoshida, S.; Iizuka, T. *Carbon* **1997**, *35*, 1031. (b) Oya, A.; Kasahara, N.; Horigome, R. *J. Mater. Sci. Lett.* **2001**, *20*, 409. (c) Lee, J.; Kim, J.; Lee, Y.; Yoon, S.; Oh, S. M.; Hyeon, T. *Chem. Mater.* **2004**, *16*, 3323.
- (15) (a) Yu, C.; Fan, J.; Tian, B.; Zhao, D.; Stucky, G. D. *Adv. Mater.* **2002**, *14*, 1742. (b) Yu, C.; Fan, J.; Tian, B.; Zhang, F.; Stucky, G. D.; Zhao, D. *Stud. Surf. Sci. Catal.* **2003**, *146*, 45.
- (16) (a) Yang, Z.; Niu, Z.; Cao, X.; Yang, Z.; Lu, Y.; Hu, Z.; Han, C. *Angew. Chem., Int. Ed.* **2003**, *42*, 4201. (b) Chae, W.-S.; Lee, S.-W.; Im, S.-J.; Moon, S.-W.; Zin, W.-C.; Lee, J.-K.; Kim, Y.-R. *Chem. Commun.* **2004**, 2554. (c) Chae, W.-S.; Lee, S.-W.; An, M.-J.; Choi, K.-H.; Moon, S.-W.; Zin, W.-C.; Jung, J.-S.; Kim, Y.-R. *Chem. Mater.* **2005**, *17*, 5651. (d) Wang, D.; Kou, R.; Yang, Z.; He, J.; Yang, Z.; Lu, Y. *Chem. Commun.* **2005**, 166.
- (17) (a) Yamaguchi, A.; Uejo, F.; Yoda, T.; Uchida, T.; Tanamura, Y.; Yamashita, T.; Teramae, N. *Nat. Mater.* **2004**, *3*, 337. (b) Lu, Q.; Gao, F.; Komarneni, S.; Mallouk, T. E. *J. Am. Chem. Soc.* **2004**, *126*, 8650. (c) Yao, B.; Fleming, D.; Morris, M. A.; Lawrence, S. E. *Chem. Mater.* **2004**, *16*, 4851.

(18) (a) Marlow, F.; Spliethoff, B.; Tesche, B.; Zhao, D. *Adv. Mater.* **2000**, *12*, 961. (b) Marlow, F.; Kleitz, F. *Microporous Mesoporous Mater.* **2001**, *44–45*, 671. (c) Wang, J.; Tsung, C.-K.; Hong, W.; Wu, Y.; Tang, J.; Stucky, G. D. *Chem. Mater.* **2004**, *16*, 5169.

(19) (a) Lee, J.-O.; Kim, J.-J.; Kim, J.; Park, J. W.; Yoo, K.-H. *J. Phys. D* **2000**, *1953*, 1956. (b) Kim, J.; Lee, J.-O.; Oh, H.; Yoo, K.-H.; Kim, J.-J. *Phys. Rev. B* **2001**, *64*, R161404. (c) Park, J. W.; Kim, J.; Lee, J.-O.; Kang, K. C.; Kim, J.-J.; Yoo, K.-H. *Appl. Phys. Lett.* **2002**, *80*, 133.

(20) (a) Kruk, M.; Jaroniec, M.; Kim, T.-W.; Ryoo, R. *Chem. Mater.* **2003**, *15*, 2815. (b) Xia, Y.; Mokaya, R. *Chem. Mater.* **2005**, *17*, 1553.

(21) Tuinstra, F.; Koenig, J. L. *J. Chem. Phys.* **1970**, *53*, 1126.

(22) (a) Matthews, M. J.; Pimenta, M. A.; Dresselhaus, G.; Dresselhaus, M. S.; Endo, M. *Phys. Rev. B* **1999**, *59*, R6585. (b) Ferrari, A. C.; Robertson, J. *Phys. Rev. B* **2000**, *61*, 14095.